Biophysical Chemistry, 43 (1992) 149–156
Elsevier Science Publishers B.V., Amsterdam

BIOCHE 01658

Isoelectric point of an ion-penetrable membrane

Toshinori Shinagawa, Hiroyuki Ohshima and Tamotsu Kondo

Faculty of Pharmaceutical Sciences and Institute of Colloid and Interface Science, Science University of Tokyo, Shinjuku-ku, Tokyo 162 (Japan)

(Received 12 September 1991; accepted in revised form 6 January 1992)

Abstract

The surface potential of an ion-penetrable planar membrane is calculated for the case in which acidic and basic groups are present in the membrane. It is found that when both acidic and basic groups are not uniformly distributed in the direction normal to the membrane, the isoelectric point (the pH value at which the surface potential becomes zero) of the membrane varies with the electrolyte concentration, whereas if both groups are uniformly distributed, the isoelectric point is independent of the electrolyte concentration. As a simple example, we treat a membrane consisting of two layers, in which acidic groups are distributed in the outer layer and basic groups are in the inner layer. Simple equations determining the membrane surface potential as a function of pH and electrolyte concentration and the dependence of the isoelectric point on the electrolyte concentration are presented.

Keywords: Isoelectric point; Ion-penetrable membrane

1. Introduction

Surface potential of charged particles or membranes immersed in an electrolyte solution plays an important role in various interfacial phenomena such as ion binding and electrostatic interaction between ions and membranes ([1,2], see also the recent review on membranes by Cevc [3]). We have recently calculated the potential distribution across ion-penetrable membranes and derived the relationship between the membrane surface potential and the density of the membrane-fixed charges for various cases, demonstrating the fundamental role of the Donnan potential [4–8]. In contrast to the case of ion-impenetrable solid surfaces, the surface potential of ion-penetrable membranes is determined not only by the membrane fixed-charges located only at the membrane surface but also by internal fixed-charges located through the region of depth of order $1/\kappa$ from the membrane surface (κ is the Debye–Hückel parameter given later by eq. 22). For this reason the surface potential of an ion-penetrable membrane generally depends on the electrolyte concentration. If, for example, the membrane-fixed charges are negative in the shallow interior of the membrane but positive in the deep interior, then the surface potential is negative at high electrolyte concentrations (at small $1/\kappa$) but may

---

Correspondence to: Dr. Hiroyuki Ohshima, Faculty of Pharmaceutical Sciences, Science University of Tokyo, 12 Ichigaya Funagawara-machi, Shinjuku-ku, Tokyo 162 (Japan).

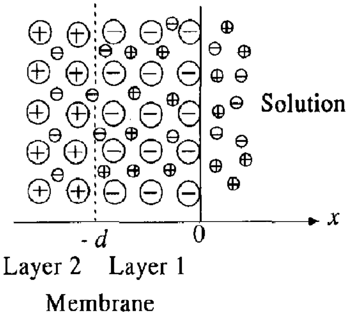

Fig. 1. Schematic representation of an ion-penetrable membrane consisting of two oppositely charged layers 1 and 2. The outer layer (layer 1) carries acidic groups and the inner layer (layer 2) basic groups. The total thickness of the membrane is much thicker than $1/\kappa$. The thickness of layer 1 is d. Membrane-fixed charges are represented by large circles with plus or minus signs, while electrolyte ions are by small circles with plus or minus signs.

become positive at low electrolyte concentrations (at large $1/\kappa$). In the present paper we shall demonstrate that the isoelectric point of an ion-penetrable membrane carrying both acidic and basic groups also depends on the electrolyte concentration if the acidic and basic groups are not uniformly distributed. In this paper we define the isoelectric point as the value of pH at which the surface potential plotted as a function of pH changes its sign. As a simple example of a membrane with non-uniform distribution of dissociated groups, we treat a membrane consisting of two layers in which the outer layer has acidic groups and the inner layer has basic groups.

2. Theory

2.1 Poisson–Boltzmann equations

Consider an ion-penetrable planar membrane consisting of two layers 1 and 2 (Fig. 1). The membrane is in equilibrium with a monovalent electrolyte solution of bulk concentration n. Note here that n represents the total concentration of monovalent cations including H^+ ions and that of monovalent anions including OH^- ions. Let n_H be the H^+ concentration in the bulk solution phase. The membrane is assumed to be much thicker than $1/\kappa$, so that it can be regarded as infinitely thick for mathematical convenience. The thickness of the outer layer is denoted as d. We take an x-axis perpendicular to the membrane surface with its origin at the membrane surface so that the region $x > 0$ is the solution phase and $x < 0$ is the membrane phase.

In the outer layer (layer 1) monovalent acidic groups of dissociation constant K_a are distributed at a density N_1 while in the inner layer (layer 2) monovalent basic groups of dissociation constant K_b are distributed at a density N_2. The mass action law for the dissociation of acidic groups AH ($AH \rightleftharpoons A^- + H^+$) gives the number density of dissociated groups, viz.,

$$\frac{N_1}{1+\dfrac{n_H}{K_a}\exp\left[-\dfrac{e\Psi(x)}{kT}\right]}. \tag{1}$$

Here $\Psi(x)$ is the electric potential at position x relative to the bulk solution phase, where $\Psi(x)$ is set equal to zero, $n_H \exp[-e\Psi(x)/kT]$ is the H^+ concentration at position x, e is the elementary electric charge, k is the Boltzmann constant and T is the absolute temperature. The charge density resulting from dissociated acidic groups at position x in layer 1($-d < x < 0$) is thus obtained by multiplying eq. (1) by $-e$, viz.,

$$-\frac{eN_1}{1+\dfrac{n_H}{K_a}\exp\left[-\dfrac{e\Psi(x)}{kT}\right]}. \tag{2}$$

Similarly, the charge density resulting from the dissociated basic groups at x in layer 2 ($x < -d$) is given by

$$+\frac{eN_2}{1+\dfrac{K_b}{n_H}\exp\left[+\dfrac{e\Psi(x)}{kT}\right]}. \tag{3}$$

The Poisson–Boltzmann equation for $\Psi(x)$ in layer 1 is then given by

$$\frac{\mathrm{d}^2\Psi}{\mathrm{d}x^2} = \frac{2en}{\varepsilon_r\varepsilon_0}\sinh\frac{e\Psi}{kT} + \frac{e}{\varepsilon_r\varepsilon_0}\frac{N_1}{1+\dfrac{n_H}{K_a}\exp\left(-\dfrac{e\Psi}{kT}\right)},$$

$$-d<x<0, \tag{4}$$

and for that in layer 2

$$\frac{\mathrm{d}^2\Psi}{\mathrm{d}x^2} = \frac{2en}{\varepsilon_r\varepsilon_0}\sinh\frac{e\Psi}{kT} - \frac{e}{\varepsilon_r\varepsilon_0}\frac{N_2}{1+\dfrac{K_b}{n_H}\exp\left(+\dfrac{e\Psi}{kT}\right)},$$

$$x<-d, \tag{5}$$

where ε_r is the relative permittivity of the electrolyte solution and ε_0 is the permittivity of a vacuum. The first term on the right-hand side of each of eqs. (4) and (5) arises from the charges of electrolyte ions. For the solution phase ($x>0$) we have

$$\frac{\mathrm{d}^2\Psi}{\mathrm{d}x^2} = \frac{2en}{\varepsilon_r\varepsilon_0}\sinh\frac{e\Psi}{kT}, \qquad x>0. \tag{6}$$

The boundary conditions are

$$\Psi(-0) = \Psi(+0), \tag{7}$$

$$\Psi(-d-0) = \Psi(-d+0), \tag{8}$$

$$\left.\frac{\mathrm{d}\Psi}{\mathrm{d}x}\right|_{x=-0} = \left.\frac{\mathrm{d}\Psi}{\mathrm{d}x}\right|_{x=+0}, \tag{9}$$

$$\left.\frac{\mathrm{d}\Psi}{\mathrm{d}x}\right|_{x=-d-0} = \left.\frac{\mathrm{d}\Psi}{\mathrm{d}x}\right|_{x=-d+0}. \tag{10}$$

These equations are continuity conditions of $\Psi(x)$ and $\mathrm{d}\Psi(x)/\mathrm{d}x$ and $x=0$ and $x=-d$.

2.2 Quasi-linearization approximation

Coupled equations for $\Psi(x)$, eqs. (4)–(6), subject to the boundary conditions, eqs. (7)–(10), can be only numerically solved. We thus employ the following quasi-linearization approximation method for obtaining the potential in the membrane interior. This method is based on the idea that the difference between the potential $\Psi(x)$ at position x in layer 1 (or 2) and the Donnan potential of layer 1 (or 2) is not large so that the Poisson–Boltzmann equation for layer 1 (or 2) can be linearized with respect to this potential difference. The maximum relative error of this method is less than 4% for the simplest case in which the two sublayers are identical and the ionizable groups are completely dissociated [8]. The Donnan potentials of layers 1 and 2, which we denote by Ψ_{D1} and Ψ_{D2}, respectively, are obtained by setting the right-hand side of the Poisson–Boltzmann equations for the respective layers, eqs. (4) and (5), equal to zero. That is, they are the solutions to the following transcendental equations:

$$\sinh(y_{D1}) + \frac{N_1}{2n}\frac{1}{1+\dfrac{n_H}{K_a}\exp(-y_{D1})} = 0, \tag{11}$$

$$\sinh(y_{D2}) - \frac{N_2}{2n}\frac{1}{1+\dfrac{K_b}{n_H}\exp(+y_{D2})} = 0, \tag{12}$$

where

$$y_{D1} = e\Psi_{D1}/kT, \tag{13}$$

$$y_{D2} = e\Psi_{D2}/kT \tag{14}$$

are the reduced Donnan potentials. Now we put

$$\Psi(x) = \Psi_{D1} + \Delta\Psi, \qquad -d<x<0, \tag{15}$$

$$\Psi(x) = \Psi_{D2} + \Delta\Psi, \qquad x<-d, \tag{16}$$

in eqs. (4) and (5) and linearize them with respect to $\Delta\Psi$. Then we have

$$\frac{\mathrm{d}^2\Delta y}{\mathrm{d}x^2} = \kappa^2 R_1^2\,\Delta y, \qquad -d<x<0, \tag{17}$$

$$\frac{\mathrm{d}^2\,\Delta y}{\mathrm{d}x^2} = \kappa^2 R_2^2\,\Delta y, \qquad x<-d, \tag{18}$$

with

$$\Delta y = e\,\Delta\Psi/kT, \tag{19}$$

$$R_1 = \left[\cosh(y_{D1}) - \frac{\sinh(y_{D1})}{1 + \frac{K_a}{n_H}\exp(+y_{D1})}\right]^{1/2}, \tag{20}$$

$$R_2 = \left[\cosh(y_{D2}) + \frac{\sinh(y_{D2})}{1 + \frac{n_H}{K_b}\exp(-y_{D2})}\right]^{1/2}, \tag{21}$$

$$\kappa = \left(\frac{2n\nu^2e^2}{\varepsilon_r\varepsilon_0 kT}\right)^{1/2}, \tag{22}$$

where κ is The Debye–Hückel parameter. Equations (15) and (16) can now be readily solved. Equation (6), on the other hand, is integrated once to give

$$\frac{e}{kT}\frac{\mathrm{d}\Psi}{\mathrm{d}x}\bigg|_{x=+0} = -2\kappa\sinh\frac{e\Psi_0}{2kT}, \tag{23}$$

where $\Psi_0 = \Psi(0)$ is the membrane surface potential. By combining the solutions to eqs. (17), (18) and eq. (23) via eqs. (7)–(10), we obtain

$$\begin{aligned}&(y_{D1} - y_{D2}) + (y_0 - y_{D1})\\ &\quad\times\left[\cosh(R_2\kappa d) + \frac{R_1}{R_2}\sinh(R_1\kappa d)\right]\\ &\quad+ 2\sinh\left(\frac{y_0}{2}\right)\left[\frac{1}{R_1}\sinh(R_1\kappa d)\right.\\ &\quad\left.+\frac{1}{R_2}\cosh(R_1\kappa d)\right] = 0.\end{aligned} \tag{24}$$

This is the required equation determining the reduced membrane surface potential y_0 $(= e\psi_0/kT)$. Here y_{D1} and y_{D2} are the solutions to eqs. (11) and (12).

2.3 Simple expression for membrane surface potential

When y_0 is small, the transcendental equation, eq. (24), can be simplified by approximating $2\sinh(y_0/2)$ by y_0 in eq. (24) so that one can obtain an explicit expression for y_0, viz.,

$$y_0 = \frac{y_{D1}\left[\cosh(R_1\kappa d) + \frac{R_1}{R_2}\sinh(R_1\kappa d) - 1\right] + y_{D2}}{\left(1 + \frac{1}{R_2}\right)\cosh(R_1\kappa d) + \left(\frac{1}{R_1} + \frac{R_1}{R_2}\right)\sinh(R_1\kappa d)}. \tag{25}$$

Since this approximation does not require that y_{D1} and y_{D2} are also low, agreement with a more accurate expression, eq. (24) is good. The isoelectric point (I.E.P.) is defined as the pH value at which y_0 reverses its sign. As is seen from eq. (25), I.E.P. depends on the electrolyte concentration n.

In order to obtain the Donnan potentials y_{D1} and y_{D2}, one must solve numerically the transcendental equations (11) and (12). In some cases, however, approximate expressions for y_{D1} and y_{D2} can be employed, which are listed below. In the pH region in which acidic groups are almost completely dissociated, it follows from eqs. (11) and (20) that

$$\begin{aligned}y_{D1} &= -\operatorname{arcsinh}\left(\frac{N_1}{2n}\right)\\ &= -\ln\left[\frac{N_1}{2n} + \left\{\left(\frac{N_1}{2n}\right)^2 + 1\right\}^{1/2}\right],\end{aligned} \tag{26}$$

and

$$R_1 = \cosh^{1/2} y_{D1} = \left[1 + \left(\frac{N_1}{2n}\right)^2\right]^{1/4}. \tag{27}$$

Similarly, in the pH in which basic groups are almost completely dissociated, we have from eqs. (12) and (21)

$$\begin{aligned}y_{D2} &= \operatorname{arcsinh}\left(\frac{N_2}{2n}\right)\\ &= \ln\left[\frac{N_2}{2n} + \left\{\left(\frac{N_2}{2n}\right)^2 + 1\right\}^{1/2}\right],\end{aligned} \tag{28}$$

and

$$R_2 = \cosh^{1/2} y_{D2} = \left[1 + \left(\frac{N_2}{2n}\right)^2\right]^{1/4}. \tag{29}$$

At pH values near pK_a, y_{D1} becomes small so that eq. (11) and (20) can be approximated by

$$y_{D1} = -\frac{N_1}{2n}\frac{1}{1+n_H/K_a} \tag{30}$$

and $R_1 = 1$. Similarly, at pH values near pK_a, we have from eqs. (11) and (20)

$$y_{D2} = \frac{N_2}{2n}\frac{1}{1+K_b/n_H} \tag{31}$$

and $R_2 = 1$. In the pH region in which the above relations can be employed, one needs not to deal with the transcendental eqs. (11) and (12). If, further, y_{D1} and y_{D2} are small, then eq. (25) become

$$y_0 = -\frac{N_1}{4n}\frac{1-\exp(-\kappa d)}{1+n_H/K_a} + \frac{N_2}{4n}\frac{\exp(-\kappa d)}{1+K_b/n_H}. \tag{32}$$

2.4 Case of uniform distribution of dissociated groups

Finally, for comparison we give below equations determining y_0 for the case of uniform distribution of both acidic and basic groups. In this situation layers 1 and 2 become identical so that the charge density at position x takes the same form throughout the membrane interior:

$$-\frac{eN_1}{1+\dfrac{n_H}{K_a}\exp\left[-\dfrac{e\Psi(x)}{kT}\right]} + \frac{eN_2}{1+\dfrac{K_b}{n_H}\exp\left[+\dfrac{e\Psi(x)}{kT}\right]} \tag{33}$$

and the reduced Donnan potential y_D of this membrane is given by the solution to the following transcendental equation:

$$\sinh(y_D) + \frac{N_1}{2n}\frac{1}{1+\dfrac{n_H}{K_a}\exp(-y_D)} - \frac{N_2}{2n}\frac{1}{1+\dfrac{K_b}{n_H}\exp(+y_D)} = 0. \tag{34}$$

The same procedure we used in deriving eq. (25) yields

$$y_0 = \frac{R}{R+1}y_D, \tag{35}$$

where

$$R = \left[\cosh y_0 + \frac{N_1}{2N}\frac{\dfrac{n_H}{K_a}\exp(-y_0)}{\left\{1+\dfrac{n_H}{K_a}\exp(-y_0)\right\}^2} - \frac{N_2}{2N}\frac{\dfrac{K_b}{n_H}\exp(y_0)}{\left\{1+\dfrac{n_H}{K_b}\exp(-y_0)\right\}^2}\right]^{1/2}. \tag{36}$$

In this case, the sign of the membrane surface potential y_0 $(=e\Psi_0/kT)$ coincides with that of the Donnan potential y_D and becomes zero when y_D becomes zero. Namely, the H$^+$ concentration at which y_0 changes its sign is given by setting y_D equal to zero in eq. (34), viz.,

$$\frac{N_1}{2n}\frac{1}{1+n_H/K_a} - \frac{N_2}{2n}\frac{1}{1+K_b/n_H} = 0, \tag{37}$$

or

$$n_H = \frac{K_a}{2}\left[\left(\frac{N_1}{N_2}-1\right) + \left\{\left(\frac{N_1}{N_2}-1\right)^2 + 4\frac{K_bN_1}{K_aN_2}\right\}^{1/2}\right]. \tag{38}$$

The I.E.P. ($= -\log n_H$, n_H being given by eq.38) is thus independent of the electrolyte concentration, in contrast to the case of non-uniform distribution of dissociated groups.

3. Results and discussion

The purpose of the present paper has been to demonstrate that the isoelectric point (I.E.P.) of an ion-penetrable membrane in which acidic and

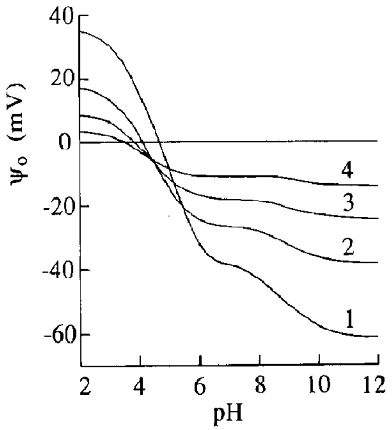

Fig. 2. Surface potential Ψ_0 of an ion-penetrable membrane consisting of two oppositely charged layers 1 and 2 as a function of pH. Calculated for $N_1 = 0.725$ *M*, $N_2 = 0.235$ *M*, $K_a = 10^{-4}$ *M* (pK_a 4), $K_b = 10^{-9}$ (pK_b 9), $T = 298$ K and $d = 0.5$ nm at several values of electrolyte concentration *n*. Curves: 1, $n = 0.02$ *M*; 2, $n = 0.05$ *M*; 3, $n = 0.1$ *M*; and 4, $n = 0.2$ *M*.

basic groups are not uniformly distributed in the membrane varies with the electrolyte concentration. We have derived equations determining the surface potential Ψ_0 and its I.E.P. of a composite membrane consisting of two oppositely charged layers, the outer layer (layer 1) carrying acidic groups and the inner layer (layer 2) carrying basic groups. Again it should be emphasized here that in the present paper by I.E.P. we mean the pH value at which the membrane surface potential changes its sign. Accordingly, at the I.E.P. the net membrane-fixed charge does not necessarily become zero. Figures 2 and 3 show the surface potential Ψ_0 as a function of pH calculated for $N_1 = 0.725$ *M*, $N_2 = 0.235$ *M*, $K_a = 10^{-4}$ *M* (pK_a = 4), $K_b = 10^{-9}$ *M* (pK_b = 9), $T = 298$ K, $d = 0.5$ nm (Fig. 2) and $d = 1$ nm (Fig. 3) at several values of the electrolyte concentration *n*. We see that the surface potential Ψ_0 and its I.E.P. (i.e., the intersection of each curve with the $\Psi_0 = 0$ axis) vary with the electrolyte concentration *n* and depend also on the thickness of the the outer layer *d*. In Fig. 4 we have replotted Ψ_0 as a function of the electrolyte concentration *n* at $d = 0.5$ nm for various values of pH. It must be noted that the membrane surface potential Ψ_0 as a function of the electrolyte concentration *n* at

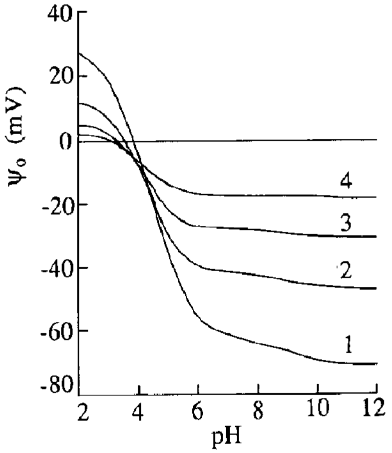

Fig. 3. Same conditions as Fig. 2, except for $d = 1$ nm.

fixed pH has an isoelectric point with respect to the electrolyte concentration, as is seen in Fig. 4. Figure 5 demonstrates the I.E.P. as a function of *n* for several values of *d*.

For comparison the corresponding results for ion-penetrable membranes with uniform distribution of acidic and basic groups are given in Fig. 6,

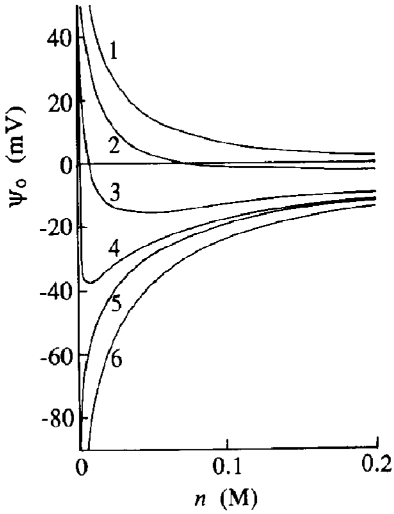

Fig. 4. Surface potential Ψ_0 of an ion-penetrable membrane consisting of two oppositely charged layers 1 and 2 as a function of electrolyte concentration *n*. Calculated for $N_1 = 0.725$ *M*, $N_2 = 0.235$ *M*, $K_a = 10^{-4}$ (pK_a 4), $K_b = 10^{-9}$ *M* (pK_b 9), $T = 298$ K and $d = 0.5$ nm at several values of pH. Curves: 1, pH 3; 2, pH 4; 3, pH 5; 4, pH 6; 5, pH 8; and 6 pH 10.

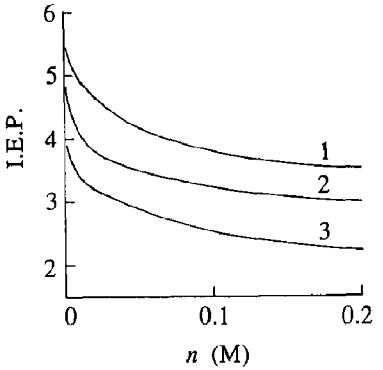

Fig. 5. Isoelectric point of of an ion-penetrable membrane consisting of two oppositely charged layers 1 and 2 as a function of the electrolyte concentration n for several values of d. Curves: 1, $d = 0.5$ nm; 2, $d = 1$ nm; and 3, $d = 2$ nm. The values of the other parameters are the same as in Figs. 2–4.

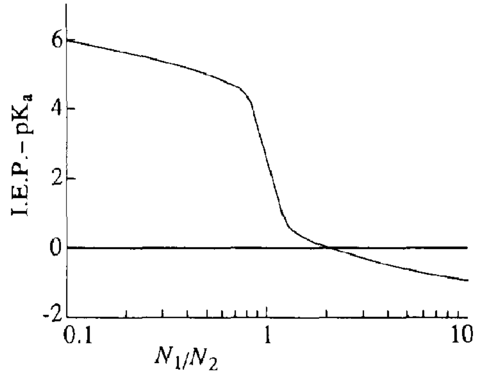

Fig. 7. The isoelectric point (I.E.P.) − pK_a of an ion-penetrable membrane with a uniform distribution of both acidic and basic groups as a function of N_1/N_2 for $K_b/K_a = 10^{-5}$.

which shows that all intersections of curves calculated for different electrolyte concentrations with the $\Psi_0 = 0$ axis are the the same. In other words, the I.E.P. of uniformly charged ion-penetrable membranes is independent of the electrolyte concentration. Figure 7 depicts the value of I.E.P. relative to pK_a as a function of N_1/N_2 for $K_b/K_a = 10^{-5}$. As should be expected, the I.E.P. shifts to higher values for lower N_1/N_2 and to lower values for larger N_1/N_2. Thus, as the density of acidic groups increases, the I.E.P. becomes small, while as the density of basic groups increases, the I.E.P. becomes high.

The dependence of the membrane surface potential Ψ_0 on the electrolyte concentration can be explained as follows. In general, the membrane surface potential is determined by the membrane fixed charges located through the depth of $1/\kappa$ from the membrane surface. Thus for moderate values of pH (curves 2–4 in Fig. 4), at high electrolyte concentration (or small $1/\kappa$) the contribution of the inner layer (layer 2) becomes small and the surface potential becomes negative. On the other hand at low electrolyte concentration (or large $1/\kappa$) the contribution from layer 2 becomes appreciable, resulting in less negative values of the membrane surface potential. With the further decrease in the electrolyte concentration Ψ_0 changes its sign. At large pH (curves 5 and 6), however, the dissociation of basic groups is weak so that the reversal in sign of Ψ_0 does not occur. At small pH (curve 3) the dissociation of acidic groups is weak so that the sign of Ψ_0 is determined by the fixed-charges of the inner layer in the concentration range shown in this figure. In all cases the surface potential suffers from shielding effects of electrolyte ions and thus tends to zero with increasing electrolyte concentration. Therefore, in curves 5–6, as the electrolyte concentration increases, the surface potential Ψ_0,

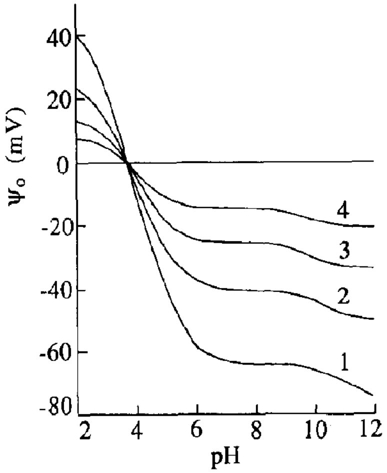

Fig. 6. Surface potential Ψ_0 of an ion-penetrable membrane with a uniform distribution of both acidic and basic groups as a function oh pH. The values of the parameters N_1, N_2, K_a, K_b and T are the same as in Figs. 2 and 3. Curves: 1, $n = 0.02$ M; 2, $n = 0.05$ M; 3, $n = 0.1$ M; and 4, $n = 0.2$ M.

after changing its sign, exhibits a minimum and then tends to zero.

Since the surface potential Ψ_0 of an ion-penetrable membrane with non-uniform distribution of acidic and basic groups depends on the electrolyte concentration, its I.E.P. also varies with the electrolyte concentration. As is seen in Fig. 5, the I.E.P. becomes lower as the electrolyte concentration n increases. The reason for this can be explained as follows via Fig. 7 for a uniformly charged ion-penetrate membrane. As the electrolyte concentrations increases ($1/\kappa$ becomes small), the contribution of the inner layer (layer 2) decreases and that of the outer layer (layer 1) increases. This corresponds effectively to an increase of the ratio of the density N_1 of the acidic groups to that of the basic groups for a uniformly charged membrane, N_1/N_2, leading to a decrease of the I.E.P. In other words, we see that increase in electrolyte concentration for a two-layered membrane effectively exhibits the same effect as increase in ratio N_1/N_2 for a uniformly charged ion-penetrable membrane.

The I.E.P. of an ion-penetrable membrane with non-uniform distribution of acidic and basic groups depends also on the thickness d of the outer layer (layer 1). As is seen in Fig. 5, the I.E.P. decreases as d increases. This dependence can also be explained via Fig. 7. Namely, the increase in d enhances the contribution from the inner layer (layer 2) and thus this effectively has the same effect as a decrease in ratio N_1/N_2 for a uniformly charged ion-penetrable membrane, resulting in a decrease in I.E.P.

In the present paper we have dealt with ion-penetrable membranes with a particular distribution of acidic and basic groups in the membrane interior. It is straightforward to extend the present treatment to other types of distribution of acidic and basic groups. The present treatment can also be applied to colloidal particles with structured surfaces, i.e., colloidal particles covered with an ion-penetrable surface charge layer composed of adsorbed polymers, such as biological cells. In such cases the surface potential Ψ_0 refers to the potential at the boundary between the surface charge layer and the surrounding solution (Fig. 8). The situation considered in the present work corresponds to the case where the surface charge layer consists of two oppositely charged sublayers. Nagahama et al. [9] have recently measured the electrophoretic mobility of guinea-pig polymorphonuclear leucocytes (PMNs) at various values of ionic strength and pH of the medium. The measured mobility is found to exhibit a behavior quite similar to that of the surface potential shown in Figs. 2 and 3 (not Fig. 6). Although the mobility is not directly proportional to the surface potential of colloidal particles with surface charge layers [10], the results obtained by Nagahama et al. [9] suggest that the surface region of guinea-pig PMNs is not uniformly charged.

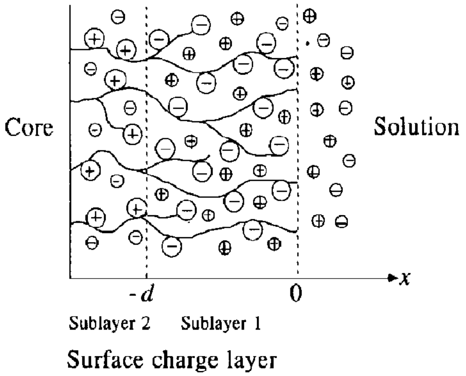

Fig. 8. A model for the cell surface covered with an ion-penetrable surface charge layer consisting of two oppositely charged sublayers 1 and 2. The outer sublayer (sublayer 1) carries acidic groups and the inner sublayer (sublayer 2) basic groups. The total thickness of the surface charge layer is much thicker than $1/\kappa$. The thickness of sublayer 1 is d.

References

1 E.J.W. Verwey and J.Th.G. Overbeek, Theory of the stability of lyophobic colloids (Elsevier, Amsterdam, 1948).
2 J.T. Davies and E.K. Rideal, Interfacial phenomena (Academic Press, New York, NY, 1961).
3 G. Cevc, Biochim. Biophys. Acta 1031-3 (1990) 311.
4 H. Ohshima and S. Ohki, Biophys. J. 47 (1985) 673.
5 H. Ohshima and T. Kondo, Colloid Polym. Sci. 264 (1986) 1080.
6 H. Ohshima and T. Kondo, J. Colloid Interface Sci. 116 (1987) 305.
7 H. Ohshima and T. Kondo, J. Theor. Biol. 124 (1987) 367.
8 H. Ohshima and T. Kondo, Biophys. Chem. 38 (1990) 117.
9 T. Nagahama, N. Muramatsu, H. Ohshima and T. Kondo, Colloids Surfaces, in press.
10 H. Ohshima and T. Kondo, Biophys. Chem. 39 (1991) 191.